Results are presented for two cases: with an overlay, assuming all cells are fully loaded with the maximum number of AMPS and/or TDMA users; and with no overlay, i.e., the transition is complete and B-CDMA users alone occupy the spectrum.

If the B-CDMA system shared the 3-sector antenna with the AMPS/TDMA system, the capacity of the B-CDMA system would be halved.

2.2 Broadband CDMA in the PCS Band

Figure 2.2 shows the variation of the capacity of a B-CDMA system as a function of data rate in the PCS band. Three curves are shown, each assuming an omnidirectional antenna in the base station. The chip rate is 12Mchips/s and the transmission bandwidth is 15MHz.

The top curve assumes no microwave users. If additional antenna sectors are employed, the number of B-CDMA users/cell increase approximately proportionally.

The next two curves represent a PCS overlay when microwave users are present. Note that the capacity in an urban area is significantly greater than in a suburban area since, in the urban area there is increased shielding between the PCS user and the microwave receiver.

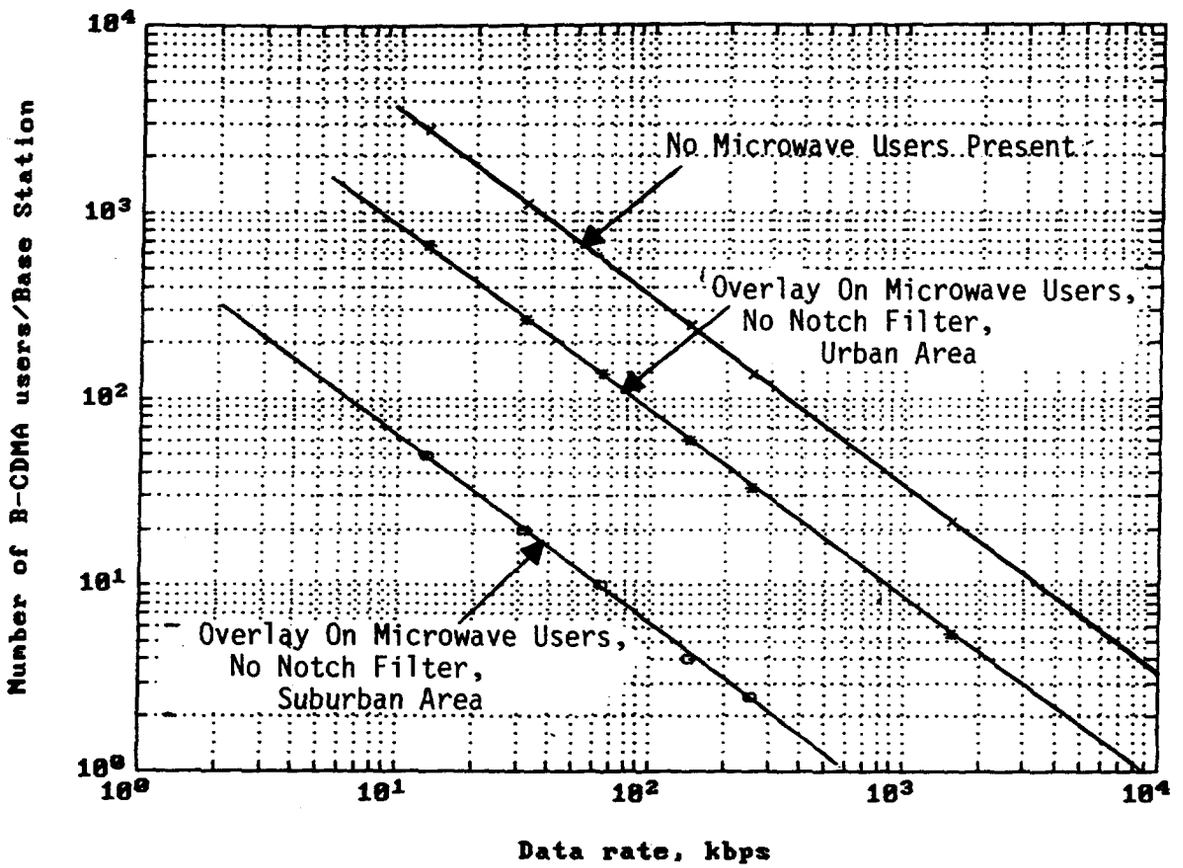

Number of B-CDMA Users in the PCS Band

FIGURE 2.2

2.3 Comparison of B-CDMA Capacity in the PcS and Cellular Bands

In order to compare the capacity of the PCS and Cellular systems, one should first note that the radius of a typical cellular cell is approximately 5000 feet while the radius of a PCS microcell is about 1000 feet. Thus the ratio of the areas serviced by a base station varies by about 25 to 1. Figures 2.1 and 2.2 compare capacity on the basis of Users/Base station, while Table 2.1 compares the PCS and cellular systems on the basis of Users/Sq. mile. Note that the number of PCS Users/Sq. mile can greatly exceed the number of Cellular Users/Sq. mile.

Data Rate, kb/s	Cellular Overlay Users/Sq. Mile		PCS Overlay Users/Sq. Mile		
	No AMPS/TDMA Users Present	AMPS/TDMA Users Present	No Microwave Users Users Present	Microwave Users Urban	Suburban
13	1,060	158	22,152	5,296	392
32	430	64	9,000	2,152	160
64	215	31	4,496	1,080	80
144	95	14	1,992	480	32
256	53	8	1,072	264	16
1,544	8	1	176	40	0

TABLE 2.1: COMPARISON OF CELLULAR AND PCS B-CDMA USERS

10.0 CONCLUSIONS

The above study shows that B-CDMA should be employed in both cellular and PcS bands in order to maximize capacity, provide high quality voice (no delays) and high data rates (up to T1).

It is further shown that through the use of microcells in the PCS band, the capacity of a PCS system, as measured in users/sq. mile, greatly exceeds the number of users/sq. mile achievable in the cellular band.

APPENDIX A

Urban/Suburban Out-Of-Sight Propagation Modeling

Urban/Suburban Out-of-Sight Propagation Modeling

Urban thoroughfares are "mean streets" for 2-GHz propagation, but a new model can help designers.

Vinko Erceg, Saeed Ghassemzadeh, Maxwell Taylor, Dong Li, and Donald L. Schilling

Due to the ever-expanding demand for personal and mobile communication networks in urban settings, it has become evident that microcellular technology must be used to accommodate more users, more efficiently. This paper focuses on the use of broadband direct sequence (DS) spread spectrum code division multiple access (CDMA) as an efficient means of communication [1-3].

There are many features of CDMA which are ideally suited for PCN, such as multipath immunity, virtually unlimited addressing, privacy without encryption, etc.

In this paper, a model is established for the calculation of the path loss characteristics of a DS Spread Spectrum Signal which occurs when a mobile user is out-of-sight of the base station due to building blockage. The environments studied are common throughout the world. For the experiments, the base station antenna was set at heights of 6.6 meters or 3.3 meters, while the mobile antenna was fixed at a height of 1.5 meters.

Out-of-Sight Communication

Out-of-sight communication is defined by Fig. 1 which illustrates a transmitter, street configuration, and a receiver moving out of sight of the transmitter. The urban area experimental data was gathered on two locations in the midtown section of New York City, with the locations of the transmitting antenna along Park and 6th avenues. The buildings in these regions are located next to each other and the average height of each building is approximately 30 meters. Each block is approximately 75 meters long. The width of the main streets and side streets are approximately 30 meters and 20 meters, respectively.

The suburban area experimental data was gathered in Flushing, New York, with the location of the transmitting antenna along Northern Boulevard. The main difference between the two environments is the relative heights of the buildings and the congestion. The Flushing buildings are approximately 15 meters in height.

For all measurements, the height of the transmitting antenna remained fixed at 6.6 meters, except for the Park Avenue measurements where a 3.3 meter transmitting antenna height was also used. The base station antenna and the transmitting equipment were placed about 4 meters away from the buildings for the 6th Avenue and Northern Boulevard measurements, while for the Park Avenue South measurements the transmitting antenna was placed in the middle of the street. The receiving antenna was mounted on the roof of a vehicle which carried the measuring equipment. A DS-BPSK Spread Spectrum signal was then transmitted from the base station at 1956 MHz and at a chip rate of 24 Mb/s. A photo interrupter placed on the measuring wheel was used as a switch to collect data at 1 cm intervals. The data was then stored on the computer's hard drive for future analysis. Omnidirectional antennas with $\lambda/4$ dipoles were used. The equipment used was manufactured by SCS Mobilecom, Inc.

LOS Model

In the line-of-sight (LOS), propagation path loss can be characterized by two slopes and a single breakpoint [1,2,4,5]. An approximate upper bound (where propagation loss is treated as a positive quantity) has been modeled [2] theoretically and verified by experimental data as

$$L_u = L_b + \begin{cases} 20\log_{10}(d/R_b), & d \le R_b \\ 40\log_{10}(d/R_b), & d > R_b \end{cases} \quad (1)$$

where d is the distance from the transmitting antenna to the receiving antenna.

An approximate lower bound [2] is given by

$$L_l = L_b + 20 + \begin{cases} 25\log_{10}(d/R_b), & d \le R_b \\ 40\log_{10}(d/R_b), & d > R_b \end{cases} \quad (2)$$

where R_b is the breakpoint in the bound and is given by

VINKO ERCEG is working toward his Ph.D. degree at the City University of New York, and is a lecturer/research assistant at the City College of New York.

SAEED GHASSEMZADEH is working toward his Ph.D. degree and is a lecturer/research assistant at the City College of New York.

MAXWELL M. TAYLOR is a university fellow at the City University of New York.

DONG LI is a lecturer/research assistant at the City College of New York.

DONALD L. SCHILLING is the Herbert G. Kayser Distinguished Professor of Electrical Engineering at the City College of New York, and president of SCS Telecom, Inc./SCS Mobilecom, Inc.

0163-6804/92/$03.00 1992© IEEE

$$R_b = \frac{4h_b h_m}{\lambda} \quad (3)$$

where h_b is the height of the transmitting antenna, h_m is the height of the mobile antenna and λ is the wavelength.

L_b is defined as

$$L_b = \left| 20 \log_{10} \left(\frac{\lambda^2}{8\pi h_b h_m} \right) \right| \quad (4)$$

These two bounds are shown in Figs. 2 and 3. Data for these figures were taken in the midtown section of New York City and Flushing, Long Island.

Out-of-Sight Path Loss Model

The out-of-sight propagation model in urban and suburban areas with perpendicular streets and avenues has two distinct characteristics. The first characteristic is that after turning the corner, a sudden drop in power level occurs. The second characteristic is that there is a steeper slope (path loss vs. distance) along the out-of-sight streets. Similar results were obtained in the Tokyo metropolitan area for the narrowband signal [7]. Both the power level drop and the steeper slopes depend on the widths of the streets and the distance from the transmitter to the corner where the mobile receiver moves out of sight (turning corner distance). As the turning corner distance increases, the power level drop and the slope also increase. The reason that this drop and different slope occurs, is because of the angles at which the reflected rays enter the out-of-sight streets as well as the number of rays entering the out-of-sight streets.

Figure 4 shows how the reflected waves enter the out-of-sight street at near and far distances. From the figure we can see that the angle δ in the out-of-sight street is larger in the case of the farther out-of-sight street. This results in more reflections along the same distance when compared to the closer out-of-sight streets. The multiple reflections are the main reason for the steeper slopes. There is a greater power loss inflicted on a ray when it bounces off the building than the loss which occurs because of the increased path length, especially for the large angles. Depending on the number of reflections along the particular distance, the path loss vs. distance slope increases. More reflections produce steeper slopes.

To develop the theoretical model, it was assumed that the reflected rays are dominant over the diffraction rays. In Fig. 4, at each point along the distance d_2, many rays contribute to the received power. When d_2 is smaller, rays which are reflected less frequently along the walls of distance d_1, are the dominant ones. As distance d_2 increases, these rays attenuate faster than the rays which are reflected frequently along the distance d_1. The rays which are reflected more frequently along the distance d_1 are less frequently reflected along the distance d_2, and as the distance d_2 increases these rays at some point experience less attenuation than the rays which are reflected

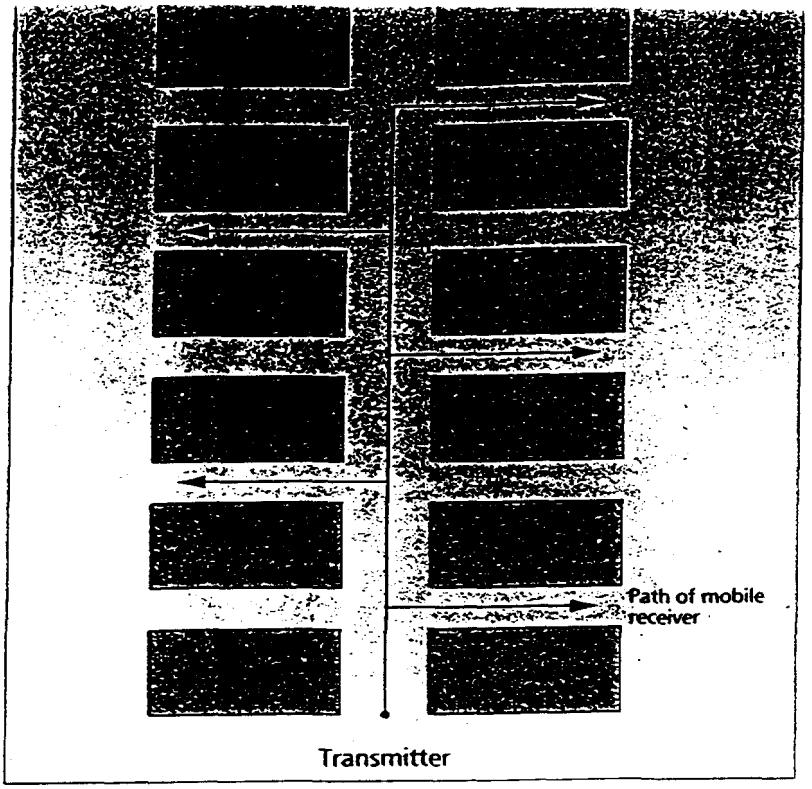

Figure 1. *Out-of-sight propagation.*

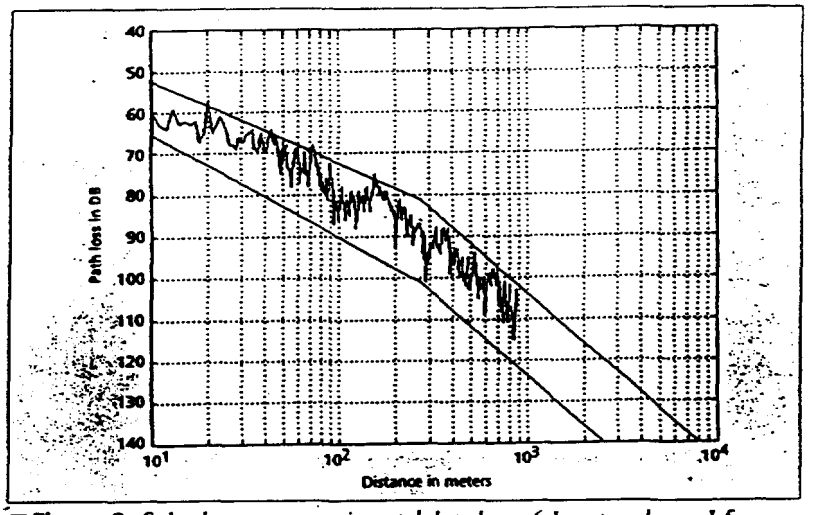

Figure 2. *Suburban-area experimental data $h_b = 6.1$ meters, $h_m = 1.5$*

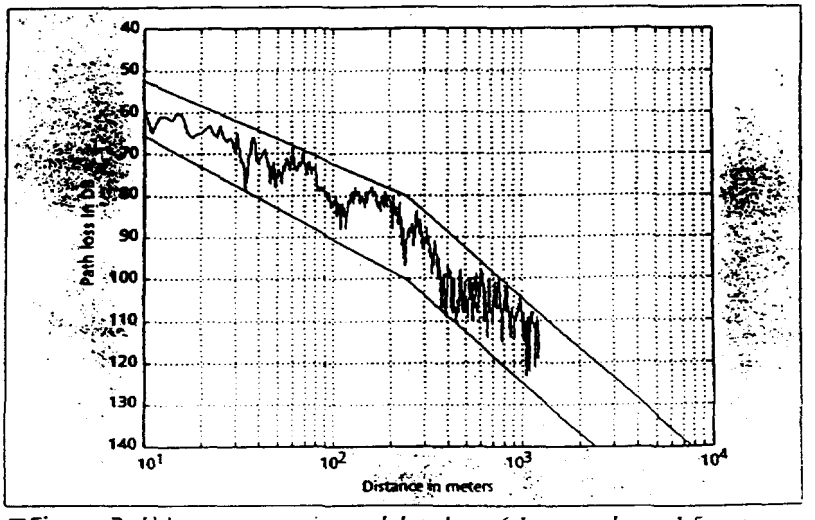

Figure 3. *Urban-area experimental data $h_b = 6.1$ meters, $h_m = 1.5$ meters.*

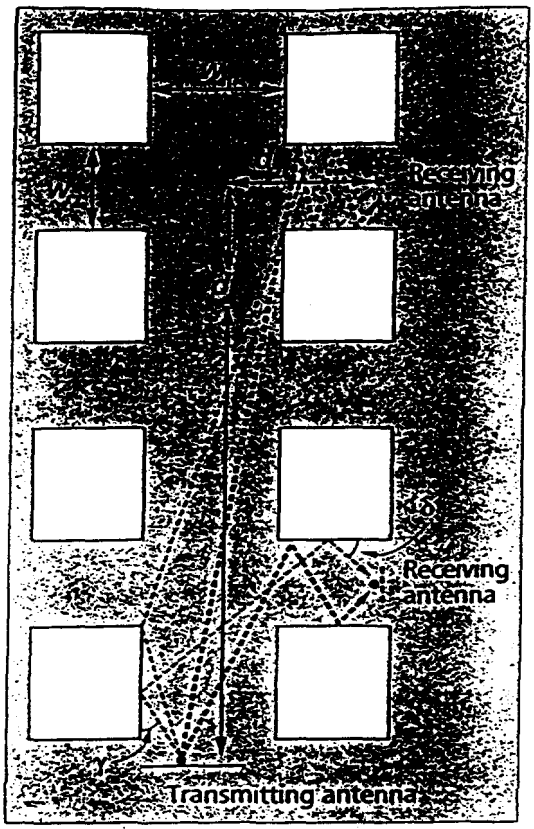

■ **Figure 4.** *Rays entering out-of-sight streets.*

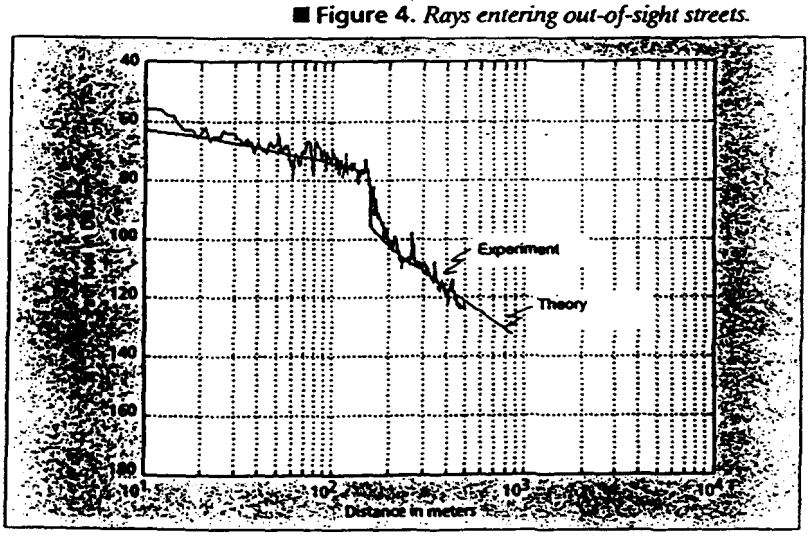

■ **Figure 7.** *Manhattan, out-of-sight propagation (d_1 = 160 meters, h_b = 6.6 meters.)*

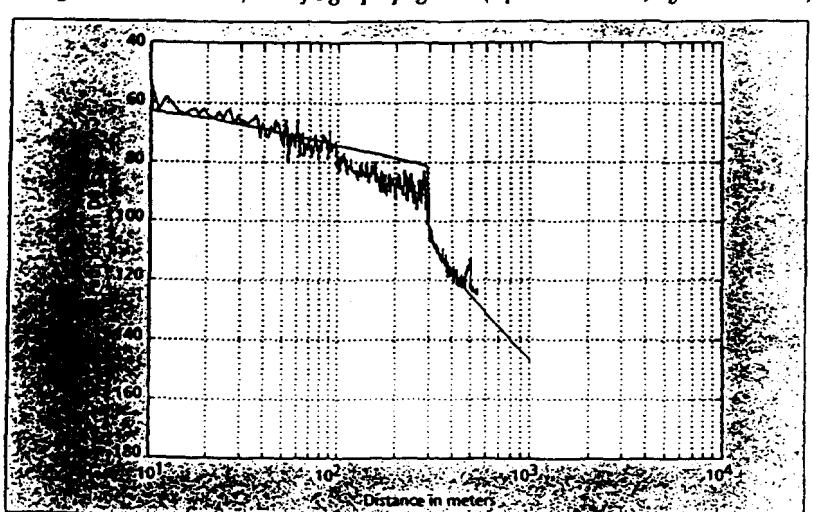

■ **Figure 8.** *Manhattan, out-of-sight propagation (d_1 = 290 meters, h_b = 6.6 meters.)*

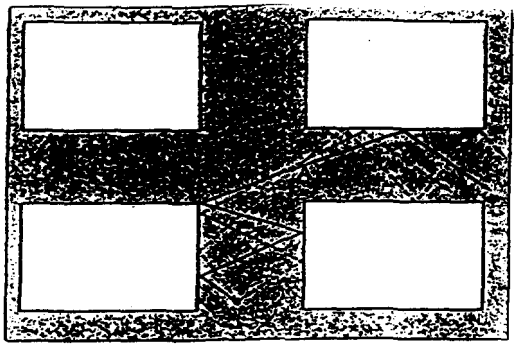

■ **Figure 5.** *Only the rays passing through point A are summed.*

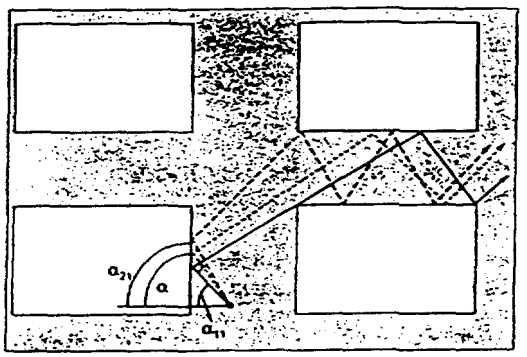

■ **Figure 6.** *Rays with the minimum angle α_{11} and the maximum angle α_{21} of rays which leave the transmitter and which enter the out-of-sight street.*

many times along the distance d_2. The power of each ray can be calculated using the classical square law propagation formula:

$$P_r = P_t\left(\frac{\lambda}{4\pi}\right)^2 \frac{R^2}{D^2} \qquad (5)$$

Where R is the total reflection coefficient and is equal to

$$R = R^N(\gamma)R^M(\delta) \qquad (6)$$

For the electric field perpendicular to the incidence plain

$$R(\gamma,\delta) = \frac{\sin(\gamma,\delta) - \sqrt{\varepsilon - \cos^2(\gamma,\delta)}}{\sin(\gamma,\delta) + \sqrt{\varepsilon - \cos^2(\gamma,\delta)}} \qquad (7a)$$

and

$$\varepsilon = \varepsilon_r - j60\sigma\lambda \qquad (7b)$$

where:

- γ is the angle between the ray and the reflecting surface in the LOS street
- δ is the angle between the ray and the reflecting surface in the out-of-sight street
- N is the number of reflections in the LOS street
- M is the number of reflections in the out-of-sight street
- D is the path length
- P_t is the transmitted power

P_r is the received power
ϵ_r is the dielectric constant
σ is the conductivity in mhos/meter

The received power of all the rays which reach the receiving antenna is calculated using

$$P_r = \sum_{i=1}^{n}\left(\frac{\lambda}{4\pi}\right)^2 \frac{R_i^2}{D_i^2} P_i + \sum_{i=1,\dots}^{n}\sum_{j=1}^{n}\left(\frac{\lambda}{4\pi}\right)^2 \frac{R_i R_j}{D_i D_j}\cos(\Delta_i - \Delta_j) P_i \tag{8}$$

where n is the number of rays reaching the antenna and $(\Delta i - \Delta j)$ is the phase difference between two rays.

In the model for out-of-sight transmission, for simplicity, only the rays which passed through point A in Fig. 5 were summed. Figure 6 shows the angle α_{11} which represents the minimum angle for which the ray leaving the transmitting antenna enters the out-of-sight street with only one reflection along the distance d_1. The angle α_{21} represents the maximum angle for such a ray. The angle α is the angle for which the ray passes through point A. Assuming that they reach the receiving antenna, the path length and the angle of incidence of the rays passing through the point A represent the approximate path length and angle of incidence while propagating along the out-of-sight street.

Now, let us define coefficient α_i as

$$\alpha_i = \frac{\alpha_{2i} - \alpha_{1i}}{\pi} \quad , i = 1, 2 \dots n \tag{9}$$

The coefficient α_i is proportional to the number of rays entering the out-of-sight street and $\alpha_i \leq 1$. The same coefficient can be calculated for each of the rays passing through point A in Fig. 5. For the LOS case $\alpha_i = 1$. The second summation term in Equation 8 represents multipath fading (the phase angles are assumed to be statistically independent having a uniform probability density function in the interval $[0 - 2\pi]$), and hence the average path loss L_r for the out-of-sight communication model is

$$L_r = \left| 10 \log_{10}\left\{ \sum_{i=1}^{n}\left(\frac{\lambda}{4\pi}\right)^2 \frac{R_i^2}{D_i^2}\alpha_i \right\} \right| \quad , \alpha_i \leq 1 \tag{10}$$

Figures 7 through 9 show the theoretical results for different turning corner distances obtained using Equation 10 as well as experimental data. The dielectric constant $\epsilon = 15$ and conductivity constant $\sigma = 7$ were used. The conductivity σ can have very large values ($>>1$) for building surfaces and structures [6].

The value of σ was chosen to give a close match to the path loss experimental data. In the theoretical analysis it was assumed that for each out-of-sight street of interest, the power leakages through the preceding streets are negligible. This assumption was based on the fact that coefficient α_i in the LOS street is 1, while in the out-of-sight street it is much less than 1, which indicates that the power leakage through the out-of-sight streets is negligible, especially when the turning corner distances are large.

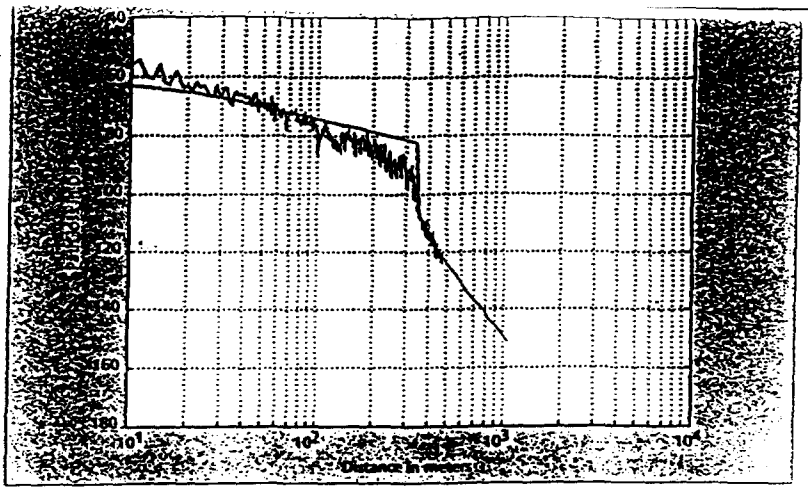

■ Figure 9. *Manhattan, out-of-sight propagation (d_1 = 360 m, h_b = 6.6 m)*

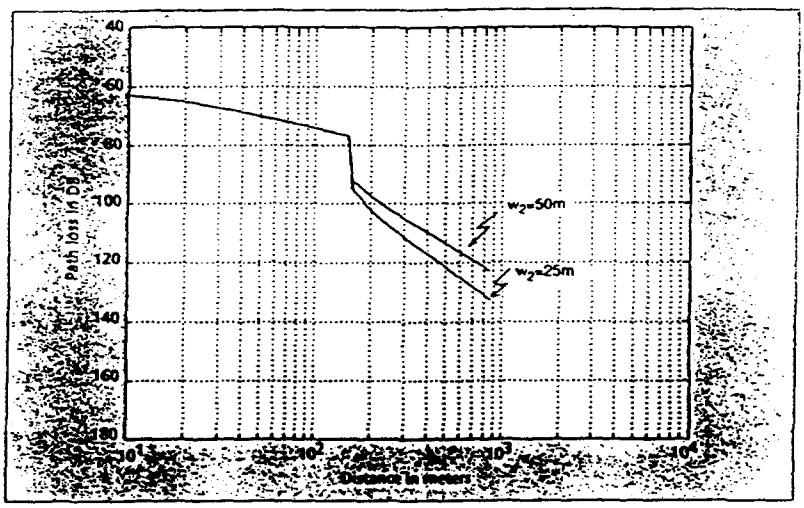

■ Figure 10. *Out-of-sight propagation (computer evaluation) for d_1 = 160 meters, w_1 = 25 meters and w_2 = 50 meters.*

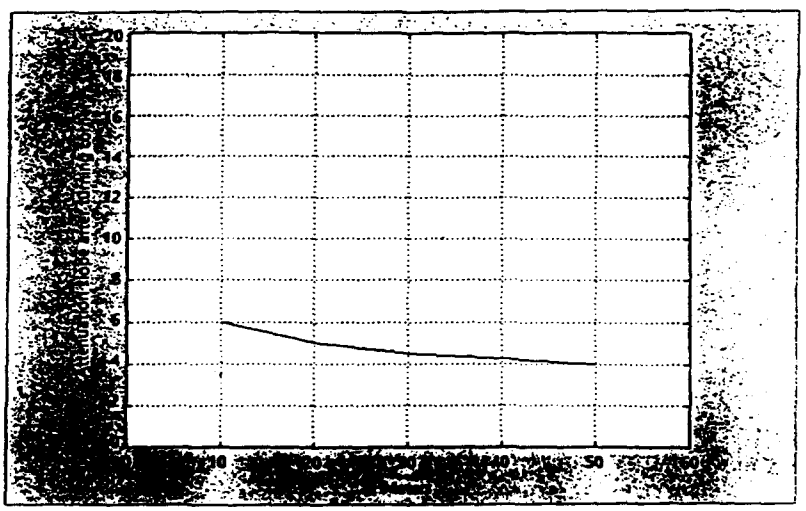

■ Figure 11. *Out-of-sight propagation (computer evaluation for the corner attenuation) d_1 = 160 meters, w_2 = 10 to 50 meters.*

Figures 13 and 14 show the corner attenuation and the slope after turning the corner as a function of the distance between the transmitter and the corner where the mobile receiver moved out-of-sight. The theoretical result obtained when the out-of-

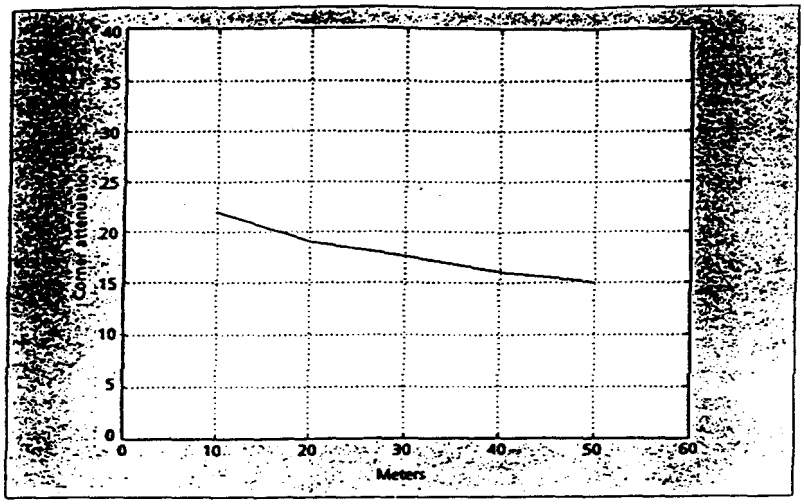

■ **Figure 12.** *Out-of-sight propagation (computer evaluation for the slope) d_1 = 160 meters, w_2 = 10 to 50 meters.*

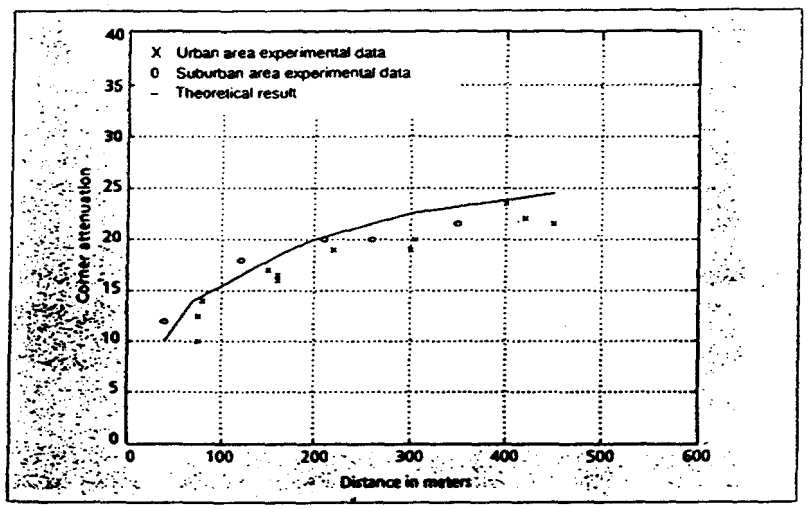

■ **Figure 13.** *All of the urban and suburban experimental data plotted together with the theoretical result for the turning corner attenuation.*

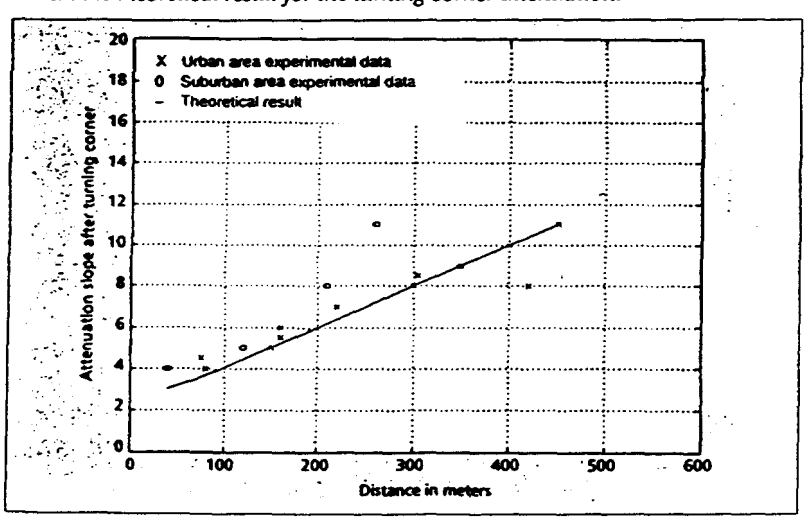

■ **Figure 14.** *All of the urban and suburban experimental data plotted together with the theoretical result for the attenuation vs. distance slope.*

sight street width was doubled is shown in Fig. 10. As expected, the corner attenuation and the slope decreased. The number of reflections in the wider out-of-sight street decreased when compared to the narrow out-of-sight street for the same distance.

Figures 11 and 12 show how the corner attenuation and the slope (attenuation vs. distance) changed when the turning corner distance and the LOS street width were kept constant at 160 meters and 30 meters, respectively, while the out-of-sight street width was varied from 10 meters to 50 meters. When the location of the transmitting antenna was changed from the middle of the street to the sidewalk, the corner attenuation and the attenuation vs. distance slope changed insignificantly because the angles for which the rays enter the side streets changed very little. By moving the transmitting antenna, the distance in the street of average width changes only about 10 meters, while the distance to the first turning corner remains approximately 75 meters (the length of the average block). However, by changing the transmitting and receiving antenna heights, LOS propagation is affected, but the corner attenuation and the attenuation vs. distance slope in the out-of-sight street remain approximately the same. Again, the reason for this is a minimal change of the angles and the path lengths of the rays which enter the side streets when the antenna heights are varied.

The average path loss equation for the out-of-sight street can be calculated using

$$L_o = L_F + A + (10B)\log_{10}\left(\frac{d_2 + d_1}{d_1}\right) \quad (11)$$

where L_F is calculated using the free space propagation formula:

$$L_F = \left|20\log_{10}\left(\frac{\lambda}{4\pi d_1}\right)\right| \quad (12)$$

where:

L_o is the path loss in the out-of-sight street

A is the corner attenuation and is determined by L_r

$A = L_r$ (immediately after turning the corner) - L_r (just before turning the corner)

B is the slope in the out-of-sight street and is determined by the slope of L_r

d_1 is the distance to the corner

d_2 is the distance along the out-of-sight street

The above equation combined with Equations 1 and 2 fully describe the LOS and out-of-sight propagation in urban and suburban environments.

Experimental Results

Extensive propagation measurements were performed in urban and suburban areas. Each of the measurements were started from the transmitting antenna into the LOS street and then a turn was made in an out-of-sight street. The sudden power level drop at the corner and the different propagation slope occurred which agreed with the theoretical model. With an increase in the distance between the transmitter and the receiver at the turning corner, both the power level drop and the slope also increased.

Figures 13 and 14 compare the power level drops (relative to the free space propagation) and the slopes as a function of distance between the transmitter and the turning corner of all the experimental data to the theoretical results. We also observe that the corner attenuation and the slope are very similar in the urban and suburban areas, which indicates that the same model can be used for both environments. The reason for this is that the heights of the antennas were considerably below the relative heights of the buildings. Additionally, the widths of the streets and the lengths of the blocks were similar. Also, while moving along the out-of-sight streets, the signal power level increased at each of the intersections because of the power coming from the other streets.

Conclusion

The results depicted here indicate that the multi-reflection model explains the power loss along the out-of-sight streets. As the turning corner distance increases, the corner attenuation and the slope also increase. Extensive propagation measurements were performed to verify the theoretical results, and it was found that the experimental results are similar in urban and suburban areas. The theoretical model also predicts how the sudden power drop and the attenuation vs. distance slope decrease as the width of the out-of-sight street increases. The corner attenuation and the slope in the out-of-sight streets are not significantly affected by the different antenna heights and locations of the transmitting antenna in the microcellular environment.

References

[1] D. L. Schilling, *et al.*, "Field Test Experiments Using Broadband Code Division Multiple Access," *IEEE Commun. Mag.*, Nov. 1991.

[2] L. B. Milstein, *et al.*, "On the Feasibility of a CDMA Overlay for Personal Communications Networks," *IEEE J. Sel. Areas Commun.*, May 1992.

[3] R. L. Pickholtz, L. B. Milstein, and D. L. Schilling, "Spread Spectrum for Mobile Communications," *IEEE Trans. Vehic. Tech.*, May 1991.

[4] E. Green and M. Hata, "Microcellular Propagation Measurements in an Urban Environment," IEEE Int'l Symp. on Personal, Indoor and Mobile Radio Commun., Sept. 1991.

[5] P. Harley, "Short Distance Attenuation Measurements at 900 MHz and 1.88 GHz Using Four Antenna Heights for Microcells," *IEEE J. Sel. Areas Commun.*, Jan. 1989.

[6] W. C. Y. Lee, *Mobile Communications Engineering*, p. 93 (McGraw Hill, 1982).

[7] Y. Nagata, *et al.*, "Measurement and Modeling of 2 GHz-Band Out-of-Sight Radio Propagation Characteristics Under Microcellular Environments," IEEE Int'l Symp. on Personal, Indoor and Mobile Radio Commun., Sept. 1991.

Biography

VINKO ERCEG received B.E. and M.E. degrees in electrical engineering from City College of New York in 1988 and 1991, respectively. Currently he is working toward his Ph.D. degree at the City University of New York, and is a lecturer/research assistant at CCNY. He is employed with SCS Mobilecom in Port Washington, New York.

SAEED GHASSEMZADEH received B.E. and M.E. degrees in electrical engineering from the City College of the City University of New York in 1989 and 1991, respectively. Currently, he is working toward his Ph.D. degree. Ghassemzadeh was program administrator for National Language Support for IBM Latin America Headquarters. At present he is a lecturer/research assistant at the City College of the City University of New York.

DONG LI received B.E. and M.E. degrees in electrical engineering from the City College of the City University of New York in 1987 and 1988, respectively. Li is a lecturer/research assistant at the City College of New York. He also is a consultant for SCS Mobilecom, Inc.

MAXWELL M. TAYLOR received the B.E. and M.E. degrees in electrical engineering from the City College of New York in 1984 and 1990, respectively. Taylor is a university fellow at the City University of New York where he is currently reading for the doctoral degree in electrical engineering.

DONALD L. SCHILLING (S'56-M'58-SM'69-F'75) is the Herbert G. Kayser Distinguished Professor of Electrical Engineering at the City College of the City University of New York where he has been a professor since 1969. Prior to that, he was a professor at the Polytechnic Institute of New York. Dr. Schilling is also President of SCS Telecom, Inc./SCS Mobilecom, Inc. In this capacity, he directs programs dealing with research and development, and training, in the military and commercial aspects of Telecommunications.

APPENDIX B

B-CDMA CELLULAR OVERLAY ON AN AMPS SYSTEM

BCDMA CELLULAR OVERLAY ON AN AMPS SYSTEM

Introduction

The following three sections prove that BCDMA with a chip rate of 10Mchips/sec can overlay on the existing AMPS system and provide an additional 496 BCDMA users to the 50 AMPS users located in the 10MHz band. If TDMA were employed rather than AMPS, then 496 BCDMA users could equally overlay the 150 TDMA users.

A major benefit of this proposed system is the transition plan. That is, there is no AMPS service reduction as the BCDMA system grows until BCDMA service exceeds 496 users. Thus, the BCDMA system could be positioned as a "business" quality service, providing privacy, bit-rate-on-demand, high quality voice and no dropped calls.

The calculations presented below assume that the AMPS system uses a 3-sector antenna system. A 6-sector system would provide increased capacity. In addition, it has been assumed that the BCDMA system uses a 6-sector antenna system. Using 3-sectors would decrease capacity.

It is important to note that the SCS Mobilecom B-CDMA cellular proposal is truly an overlay and will not noticeably affect existing AMPS or TDMA users. The SCS system will provide carriers with the ability to maximize the utilization of their scarce resource - the frequency spectrum. Incremental subscribers will be added with the B-CDMA "business" quality service. As the ratio of B-CDMA to AMPS/TDMA users increases, the

B-CDMA system will gracefully accommodate the new users.

Capacity Increase

The SCS Mobilecom system easily meets the 1988 CTIA User Performance Requirements (UPR) for 10 times AMPS capacity.

More importantly, because the transition to the next generation standard is one of the most critical factors, please review the following relative capacity increase table. Note: these capacities are derived without removing one AMPS or TDMA user.

	AMPS	B-CDMA	TOTAL	CAPACITY INCREASE FACTOR
32 kbps	50	200	250	5
13 kbps	50	496	546	11

This clearly demonstrates the robustness and flexibility of B-CDMA. During transition, using a high quality voice digitizer, B-CDMA can provide 5 times todays capacity, providing sufficient capacity for most markets through the end of the decade. As the number of existing AMPS/TDMA users convert to B-CDMA, more capacity is available as AMPS channels are turned down. Ultimately, 20 times AMPS capacity can be met if all AMPS/TDMA users are converted; all this, with a high quality 32 kbps voice coder.

1.0 Frequency Modulation

Consider the AMPS cellular user receiving the desired FM signal plus interfering B-CDMA signals. The input to the discriminator is therefore:

$$v_I(t) = \sqrt{2P_A}\cos(\omega_o t+\theta(t)) + \sum_{i=1}^{n}\sqrt{2P_C}\,c_i(t)\cos(\omega_o t+\phi_I) + n_w(t) \quad (1.1)$$

where $n_w(t)$ is thermal white gaussian noise. The FM receiver filters the interference, reducing its power by the processing gain, K, which is defined as the ratio of the spread spectrum bandwidth to the FM bandwidth. Typically K = 10MHz/30kHz = 330. The filter output is

$$v_I(t) = \sqrt{2P_A}\cos(\omega_o t+\theta(t)) + \sum_{i=1}^{n}\sqrt{2P_C/K}\,z_I(t)\cos(\omega_o t+\phi_I) + n(t) \quad (1.2)$$

where $z_i(t)$ is the chip stream $c_i(t)$ after filtering, and ϕ_i is the phase of each CDMA interferer relative to the FM carrier. The noise n(t) has been filtered.

Rice [1] has pointed out, as has Schilling [2], that the modulation $\theta(t)$ has little effect on the calculation of the output noise power in an FM output SNR calculation. Setting $\theta(t)$ equal to 0 for this calculation yields the phaser diagram shown in Fig. 1.1.

The output of an FM discriminator is the derivative of ψ with respect to time. Assuming a high input signal to noise ratio, C/I, i.e., assuming that:

$$P_A >> nP_C/K \quad (1.3)$$

and

$$\tan \psi \approx \psi \tag{1.4}$$

yields

$$\frac{d\psi}{dt} \approx \sum_{i=1}^{n} \sqrt{\frac{P_C / P_A}{K}}\, z_i(t) \sin\phi_i \tag{1.5}$$

To simplify the calculations we can assume that the heavily filtered chip stream $z_i(t)$ looks like bandlimited, white, gaussian noise, with variance equal to unity. Then, the output interfering power N_I, due to the z_i, in a bandwidth, f_m = 30kHz is [2].

$$N_I \approx n\left(\frac{P_C / P_A}{2K}\right)\frac{4\pi^2}{3B} f_m^3 \approx n\left(\frac{P_C / P_A}{2K}\right)\frac{\omega_m^2}{3} f_m / B \tag{1.6}$$

where B is the IF bandwidth. Similarly, the output power due to thermal noise is

$$N_{TH} \approx \frac{\eta}{P_A}\left(\frac{4\pi^2 f_m^3}{3}\right) \approx \frac{\eta f_m}{P_A}\left(\frac{\omega_m^2}{3}\right) \tag{1.7}$$

Assuming sinewave modulation, the output signal power is [2]

$$S_o \approx (\beta \omega_m)^2/2 \tag{1.8}$$

Hence the output signal-to-noise-ratio is

$$\frac{S_o}{N_I + N_{TH}} \approx \frac{\beta^2 \omega_m^2 / 2}{n\left(\frac{P_C / P_A}{2K}\right)\frac{\omega_m^2 f_m}{3B} + \frac{\eta f_m}{P_A}\left(\frac{\omega_m^2}{3}\right)}$$

$$- \frac{3}{2}\beta^2 (P_A/\eta f_m) \Big/ \left[1 + \frac{n}{2K}\left(\frac{P_C}{P_A}\right)\left(\frac{P_A}{\eta f_m}\right)\right] \qquad (1.9)$$

$$SNR_o - \frac{3}{2}\beta^2 (CNR)\left(\frac{B}{f_m}\right) \Big/ \left[1 + \frac{n}{2K}\left(\frac{P_C}{P_A}\right)(CNR)\right] \qquad (1.10)$$

where CNR = $(P_A/\eta B)$. For example, in our AMPS/BCDMA overlay, $\beta = 4$, $B/f_m = 10$, $K = 330$ and $P_A/P_C = 10$. Then if, for example, $n = 144$,

$$SNR_o - 240(CNR)/[1+0.22(0.1)CNR] - 240\left(\frac{CNR}{P_n}\right)/[1+0.022(CNR)] \qquad (1.11)$$

Figure 1.2 plots Eq. (1.10) for different numbers of CDMA users, n, in an AMPS antenna sector.

Figure 1.2 can also be used to estimate performance in a fading medium. For example, if the number of simultaneous B-CDMA users in an AMPS sector is 144 and if the average carrier to thermal noise ratio, CNR, seen by the AMPS system is 19dB, then the demodulated output $(SNR)_o$ of the AMPS FM demodulator is 43dB. A 6dB fade would reduce the CNR to 13dB and reduce the demodulated output SNR to 37dB.

We shall employ Eq. (1.10) in Sec. 3 to determine the maximum number of CDMA users allowable.

2.0 CDMA

Consider a CDMA system receiving a desired spread spectrum signal in the presence of interference. Since CDMA systems are interference, rather than thermal noise, limited, our discussion will neglect the thermal noise. The coherent receiver employed by SCS performs the demodulation procedure shown in Fig. 2.1. In this figure the phases θ_i and ϕ_j represent the effect of random propagation delays and are independent random variables, uniformly distributed between $-\pi$ and π. The spreading codes (chip sequences) are $c_i(t-\tau_i)$ where $\tau_i = 0$ if the chip edges would line up. Assume the chip edges occur displaced from that of user U_o by the time τ_i. Because we are using a large spreading sequence, each bit appears as though it were spread by a truly random binary sequence and thus τ_i can be assumed to be uniformly distributed between 0 and T_c, where T_c is the chip duration. The ratio T_b/T_c, which is the ratio of a data bit to a chip, is called the "processing gain". Note that this processing gain is different from the one defined in Eq. 1.2. The phase ϕ_{mj} represents the FM modulation. In the AMPS system the maximum value of ϕ_{mj} is approximately equal to 4.

Referring to Fig. 2.1 we have

$$v_o = \sqrt{2P_C}\, T_b d_o + \sqrt{2P_C}\, T_b \sum_{i=1}^{n_1} \cos\theta_i \frac{1}{T_b} \int_0^{T_b} c_o(t)\, c_i'(t-\tau_i)\, dt + \sqrt{2P_A}\, T_b \sum_{j=1}^{n_2} \frac{1}{T_b} \int_0^{T_b} c_o(t) \cos(\phi_{mj}(t) + \phi_j)\, dt \tag{2.1}$$

where

$$c_i'(t-\tau_i) = d_i(t-\tau_i)\, c_i(t-\tau_i)$$

since the c_i's are assumed random.

We shall now determine the output SNR of the CDMA system. To proceed, let us consider separately the interfering power produced by each type of interfering signal.

2.1 Interference Caused by Other CDMA Users

The interference caused by the n_1 CDMA interferers is

$$I_1 = \sqrt{2P_C} \sum_{i=1}^{n_1} \cos\theta_i \int_0^{T_b} c_o(t)\, c_i'(t-\tau_i)\, dt \qquad (2.2)$$

The power in I_1, I_1^2 is

$$\overline{I_1^2} = \frac{1}{2}(2P_C) \overline{\left[\sum_{i=1}^{n_1} \int_0^{T_b} c_o(t)\, c_i'(t-\tau_i)\, dt\right]^2} \qquad (2.3)$$

In this expression we have used the fact that

$$\overline{\cos^2\theta_i} = 1/2 \qquad (2.4)$$

It has been shown by Pursley [3] and others, that the power due to the chips not being in alignment is less than the power obtained when $\tau_i = 0$, for all i. Indeed the expression usually used is

$$\overline{\left[\sum_{i=1}^{n_1} \int_0^{T_b} c_o(t)\, c_i'(t-\tau_i)\, dt\right]^2} = \frac{2}{3} n_1 \qquad (2.5)$$

While the derivation of this result is, in general, complicated, three simple examples illustrate the point:

2.1.1 Rectangular Pulses

Consider the rectangular pulses c_o and c'_i shown in Fig 2.2.

Note that the product $c_o(t)\ c'_i(t-\tau_i)$ is

$$c_o(t)\, c_i'(t-\tau_i) = \begin{cases} \pm 1 & 0 \le t \le \tau_i, \text{ each with } P = \frac{1}{2} \\ \pm 1 & \tau_1 \le t < T_c, \text{ each with } P = \frac{1}{2} \end{cases} \qquad (2.6)$$

Therefore

$$\int_0^{T_c} c_o(t)\, c_i'(t-\tau_i)\, dt = \begin{cases} \pm T_c \text{ each with } P = \frac{1}{2} \\ \pm (T_c - \tau_i) \text{ each with } P = \frac{1}{2} \end{cases} \qquad (2.7)$$

Therefore

$$\overline{\left[\int_0^{T_c} c_o(t)\, c_i'(t-\tau_i)\, dt\right]^2} = \overline{\frac{1}{2}(T_c)^2 + \frac{1}{2}(T_c - \tau_i)^2} = \frac{2}{3} T_c^2 \qquad (2.8)$$

To obtain Eq (2.8) we assumed that τ_i was uniformly distributed between 0 and T_c. Note that if $\tau_i = 0$,

$$\int_0^{T_c} c_o(t)\, c_i'(t)\, dt = \pm T_c \text{ each with } P = \frac{1}{2}$$

and

$$\overline{\left[\int_0^{T_c} c_o(t)\, c_i'(t)\, dt\right]^2} = T_c^2 \tag{2.9}$$

Ergo, comparing Eqs. (2.8) and (2.9) yields the factor of 2/3.

2.1.2 Half-sinusoidal input pulses

A second example assumes $c'_i(t) = \sin \pi t/Tc$ and $c_o(t)$, for simplicity of calculation, is taken to be rectangular as illustrated in Fig 2.3. In this example,

$$\int_0^{T_c} c_o(t)\, c_i'(t-\tau_I)dt = \pm \frac{T_c}{\pi}\left[1 - \cos\frac{\pi\tau_I}{T_c}\right] \pm \frac{T_c}{\pi}\left[\cos\frac{\pi\tau_I}{T_c} - 1\right] \tag{2.10}$$

The average power is then

$$\overline{\left[\int_0^{T_c} c_o(t)c_i'(t-\tau_I)dt\right]^2} = \frac{1}{T_c}\int_0^{T_c}\left\{\frac{1}{2}\left(\frac{2T_c}{\pi}\right)^2 + \frac{1}{2}\left(\frac{2T_c}{\pi}\right)^2\cos^2\frac{\pi\tau_I}{T_c}\right\} d\tau_I \tag{2.11}$$

$$= \frac{3}{4}\left(\frac{2T_c}{\pi}\right)^2$$

If $\tau_i = 0$, it is readily shown that

$$\overline{\left[\int_0^{T_c} c_o(t)\, c_i'(t)\, dt\right]^2} - \left(\frac{2T_c}{\pi}\right)^2 \qquad (2.12)$$

Note the factor now becomes 3/4 rather than 2/3.

2.1.3 The Raised-Cosine

If $c'_i(t) = 1 - \cos 2\pi t/T_c$, a raised cosine, the result would be $0.8T_c^2$ compared to T_c^2 if $\tau_i=0$. The factor is now 0.8.

Since the value obtained in evaluating Eq (2.5) is dependent on the pulse shape and varies for the cases considered: 2/3 (rectangular), 3/4 (half-sinewave) and 0.8 (raised-cosine). For rectangular shape pulses, Eq. (2.3) becomes*

$$\overline{I_i^2} = \frac{T_b^2\, n_1}{3} (2P_c) \frac{f_b}{f_c} \qquad (2.13)$$

2.2 Interference Caused by the FM Users

The interference caused by the n_2 FM AMPS users is

*The factor of 3 in the denominator of Eq. (2.13) is the factor under discussion. This factor is well known and alternative derivations of the error rate in CDMA system have also obtained this factor. The most recent paper is by J. Holtzman, [4].

$$I_2 = \sqrt{2P_A}\, T_b \sum_{j=i}^{n_2} \frac{1}{T_b} \int_0^{T_b} c_o(t) \cos\left(\phi_{mj}(t) + \phi_j\right) dt \qquad (2.14)$$

To simplify the discussion we approximate Eq. (2.14) by the summation

$$I_2 = \sqrt{2P_A}\, T_c \sum_{j=1}^{n_2} \sum_{i=1}^{T_b/T_c} C_o(i\,T_c) \cos\left[\phi_{m_j}(i\,T_c) + \phi_j\right] \qquad (2.15)$$

Then the variance of I_2 becomes

$$\overline{I_2^2} = (2P_A)\, T_c^2 \sum_{j=1}^{n_2} \sum_{i=1}^{T_b/T_c} E\left\{COS^2\left[\phi_{m_j}(i\,T_c) + \phi_j\right]\right. \qquad (2.16)$$

Hence

$$\overline{I_2^2} = T_b^2\, n_2\, (P_A)\, f_b / f_c \qquad (2.17)$$

2.3 Signal-To-Noise Ratio

The SNR seen by a BCDMA user in the presence of other B-CDMA users and AMPS users is then, from Eqs. (2.1), (2.13) and (2.17):

$$SNR = \frac{2P_C\, T_b^2}{2P_C\, T_b^2 \left(\frac{n_1}{3} \cdot \frac{f_b}{f_c}\right) + 2P_A\, T_b^2 \left(\frac{n_2}{2} \cdot \frac{f_b}{f_c}\right)}$$

$$= \frac{f_c / f_b}{\frac{n_1}{3} + \frac{n_2}{2}\left(\frac{P_A}{P_C}\right)} \qquad (2.18)$$

3.0 The Cellular Overlay

Using Eq (2.17) we can explain the operation of cellular overlay.

3.1 Effect of AMPS Users on the BCDMA Base Station (Fig. 3.1)

Assuming that the BCDMA base station uses a 60 degree (6 sector) antenna, the number of interfering AMPS users is

$$n_2 = 1.6\ (50/6) = 13 \tag{3.1}$$

where 50 is the number of AMPS users in a cell, 6 is the fraction of users in the sector and the factor 1.6 includes adjacent cell interference.

The processing gain f_c/f_b = 10Mchips/s/13kbits/sec

$$\frac{f_c}{f_b} = \frac{10\ Mchips/s}{13\ kbits/s} = 770 \tag{3.2}$$

Let the ratio of the powers transmitted by the AMPS and BCDMA users be $P_A/P_C^* = 15$. Then Eq. (2.17) becomes

$$SNR = \frac{770}{\frac{n_1}{3} + \frac{13}{2}(15)} \tag{3.3}$$

If the SNR at the receiver is 6dB (=4), which is sufficient to yield an error rate of 10^{-3} (the Adaptive Delta Modulator (ADM) performs properly with a BER = 10^{-2}),

---

*$P_A \backslash P_C$ is the ratio of the power received at the base station due to an AMPS user, to the power received at the same base station due to a BCDMA user.

$$n_1 = 285 \quad (\textit{neglecting VAD}) \tag{3.4}$$

If we assume that approximately 60% of the interfering users are in the adjacent sectors of the neighboring 2 cells and since there are 6 sectors, more than (285/1.6) x 6 = 1069 CDMA users can simultaneously access the CDMA base neglecting VAD and 2137 CDMA users with VAD.

We shall see below in Sections 3.3 and 3.4, that user interference to the base station does not limit performance.

3.2 Effect of BCDMA Users on the AMPS Base Station (Fig. 3.2)

Assuming that the AMPS base station uses a 3-sector antenna, Eq. (1.10) yields the FM demodulated output SNR:

$$(SNR)_o = \frac{3}{2}\beta^2 (CNR)\left(\frac{B}{f_m}\right) \Big/ \left\{1 + \frac{n_1}{2K}\left(\frac{P_C}{P_A}\right)(CNR)\right\} \tag{3.5}$$

where CNR is the carrier power-to-thermal noise ratio.

Let $\beta = 4$, $B/f_m = 10$, $K = 330$, $P_A/P_C^* = 10$ and CNR = 17dB(50).

If we design so that the CDMA interference is equal to the thermal noise power, then

---

*P_A/P_C is the ratio of the power received at the base station due to an AMPS user to the power received at the same base station due to a BCDMA user.